Femtosecond SESAM-modelocked Cr:ZnS laser

Evgeni Sorokin,[1*] Nikolai Tolstik,[2] Kathleen I. Schaffers,[3] and Irina T. Sorokina[2]

[1]*Photonics Institute, TU Wien, Gusshausstrasse 27/387, A-1040 Vienna, Austria*
[2]*Department of Physics, Norwegian University of Science and Technology, N-7491 Trondheim, Norway*
[3]*University of California, Lawrence Livermore National Laboratory L-482, Livermore, California 94550, USA*
[*]*sorokin@tuwien.ac.at*

Abstract: We report self-starting femtosecond operation of a 180-MHz SESAM-controlled prismless Cr:ZnS laser around 2400 nm at open air and room temperature. Dispersion compensation was achieved by a combination of bulk materials and chirped mirrors. Both soliton- and chirped-pulse operation regimes have been demonstrated with 130 fs (630 fs) pulse duration at 130 (205) mW average output power, respectively. The output power was about 30% higher than for a comparable Cr:ZnSe sample in the same cavity.

OCIS codes: (140.3580) Lasers, solid-state; (140.7090) Ultrafast lasers; (140.4050) Mode-locked lasers.

References and links

1. L. D. DeLoach, R. H. Page, G. D. Wilke, S. A. Payne, and W. F. Krupke, "Transition metal-doped zinc chalcogenides: Spectroscopy and laser demonstration of a new class of gain media," IEEE J. Quantum Electron. **32**(6), 885–895 (1996).
2. I. T. Sorokina, "Cr^{2+}-doped II–VI materials for lasers and nonlinear optics," Opt. Mater. **26**(4), 395–412 (2004).
3. E. Sorokin, S. Naumov, and I. T. Sorokina, "Ultrabroadband infrared solid-state lasers," IEEE J. Sel. Top. Quantum Electron. **11**(3), 690–712 (2005).
4. R. H. Page, K. I. Schaffers, L. D. Deloach, G. D. Wilke, F. D. Patel, J. B. Tassano, Jr., S. A. Payne, W. F. Krupke, K. T. Chen, and A. Burger, "Cr^{2+}-doped zinc chalcogenides as efficient, widely tunable mid-infrared lasers," IEEE J. Quantum Electron. **33**(4), 609–619 (1997).
5. I. Sorokina, E. Sorokin, S. Mirov, V. Fedorov, V. Badikov, V. Panyutin, A. Di Lieto, and M. Tonelli, "Continuous-wave tunable Cr^{2+}:ZnS laser," Appl. Phys. B **74**(6), 607–611 (2002).
6. I. T. Sorokina, E. Sorokin, S. Mirov, V. Fedorov, V. Badikov, V. Panyutin, and K. I. Schaffers, "Broadly tunable compact continuous-wave Cr^{2+}: ZnS laser," Opt. Lett. **27**(12), 1040–1042 (2002).
7. S. B. Mirov, V. V. Fedorov, K. Graham, I. S. Moskalev, I. T. Sorokina, E. Sorokin, V. Gapontsev, D. Gapontsev, V. V. Badikov, and V. Panyutin, "Diode and fibre pumped Cr^{2+}: ZnS mid-infrared external cavity and microchip lasers," IEE Proc., Optoelectron. **150**(4), 340–345 (2003).
8. I. S. Moskalev, V. V. Fedorov, and S. B. Mirov, "10-Watt, pure continuous-wave, polycrystalline Cr^{2+}:ZnS laser," Opt. Express **17**(4), 2048–2056 (2009).
9. E. Sorokin, I. T. Sorokina, M. S. Mirov, V. V. Fedorov, I. S. Moskalev, and S. B. Mirov, "Ultrabroad Continuous-Wave Tuning of Ceramic Cr:ZnSe and Cr:ZnS Lasers," in *Advanced Solid-State Photonics 2010*, Technical Digest (CD) (Optical Society of America, 2010), paper AMC2.
10. I. T. Sorokina, "Crystalline Mid-Infrared Lasers," in *Solid-State Mid-Infrared Laser Sources*, I. T. Sorokina and K. Vodopyanov, eds. (Springer, 2003), pp. 262–358.
11. I. T. Sorokina, E. Sorokin, and T. Carrig, "Femtosecond Pulse Generation from a SESAM Mode-Locked Cr:ZnSe Laser," in *Conference on Lasers and Electro-Optics (CLEO)*, Technical Digest (CD) (Optical Society of America, 2006), paper CMQ2.
12. E. Sorokin and I. T. Sorokina, "Ultrashort-pulsed Kerr-lens modelocked Cr:ZnSe laser," in *CLEO/Europe and EQEC 2009 Conference Digest*, (Optical Society of America, 2009), paper CF1_3.
13. M. N. Cizmeciyan, H. Cankaya, A. Kurt, and A. Sennaroglu, "Kerr-lens mode-locked femtosecond Cr^{2+}:ZnSe laser at 2420 nm," Opt. Lett. **34**(20), 3056–3058 (2009).
14. E. Slobodtchikov and P. Moulton, "Progress in Ultrafast Cr:ZnSe Lasers," in *Advanced Solid-State Photonics*, OSA Technical Digest (CD) (Optical Society of America, 2012), paper AW5A.4.
15. E. Sorokin, I. T. Sorokina, J. Mandon, G. Guelachvili, and N. Picque, "Sensitive multiplex spectroscopy in the molecular fingerprint 2.4 μm region with a Cr^{2+}:ZnSe femtosecond laser," Opt. Express **15**(25), 16540–16545 (2007).

#178674 - $15.00 USD Received 26 Oct 2012; revised 26 Nov 2012; accepted 27 Nov 2012; published 12 Dec 2012

16. B. Bernhardt, E. Sorokin, P. Jacquet, R. Thon, T. Becker, I. T. Sorokina, N. Picqué, and T. W. Hänsch, "Mid-infrared dual-comb spectroscopy with 2.4 μm Cr^{2+}:ZnSe femtosecond lasers," Appl. Phys. B **100**(1), 3–8 (2010).
17. P. F. Moulton and E. Slobodchikov, "1-GW-peak-power, Cr:ZnSe laser," in *CLEO:2011 - Laser Applications to Photonic Applications*, OSA Technical Digest (CD) (Optical Society of America, 2011), paper PDPA10.
18. K. L. Vodopyanov, E. Sorokin, I. T. Sorokina, and P. G. Schunemann, "Mid-IR frequency comb source spanning 4.4-5.4 μm based on subharmonic GaAs optical parametric oscillator," Opt. Lett. **36**(12), 2275–2277 (2011).
19. I. T. Sorokina, E. Sorokin, T. J. Carrig, and K. I. Schaffers, " A SESAM Passively Mode-Locked Cr:ZnS Laser," in *Advanced Solid-State Photonics*, Technical Digest (Optical Society of America, 2006), paper TuA4.
20. C. R. Pollock, N. A. Brilliant, D. Gwin, T. J. Carrig, W. J. Alford, J. B. Heroux, W. I. Wang, I. Vurgaftman, and J. R. Meyer, "Mode locked and Q-switched Cr:ZnSe laser using a Semiconductor Saturable Absorbing Mirror (SESAM)," in *Advanced Solid-State Photonics*, Technical Digest (Optical Society of America, 2005), paper TuA6.
21. I. T. Sorokina and E. Sorokin, "Chirped-Mirror Dispersion Controlled Femtosecond Cr:ZnSe Laser," in *Advanced Solid-State Photonics*, OSA Technical Digest Series (CD) (Optical Society of America, 2007), paper WA7.
22. S. L. Schieffer, J. A. Berger, B. L. Rickman, V. P. Nayyar, and W. A. Schroeder, "Thermal effects in semiconductor saturable-absorber mirrors," J. Opt. Soc. Am. B **29**(4), 543–552 (2012).
23. D. H. Sutter, L. Gallmann, N. Matuschek, F. Morier-Genoud, V. Scheuer, G. Angelow, T. Tschudi, G. Steinmeyer, and U. Keller, "Sub-6-fs pulses from a SESAM-assisted Kerr-lens modelocked Ti:sapphire laser: At the frontiers of ultrashort pulse generation," Appl. Phys. B **70**(S1), S5–S12 (2000).
24. D. J. Ripin, J. T. Gopinath, H. M. Shen, A. A. Erchak, G. S. Petrich, L. A. Kolodziejski, F. X. Kärtner, and E. P. Ippen, "Oxidized GaAs/AlAs mirror with a quantum-well saturable absorber for ultrashort-pulse Cr^{4+}:YAG laser," Opt. Commun. **214**(1-6), 285–289 (2002).
25. E. Sorokin, N. Tolstik, and I. T. Sorokina, "Kerr-Lens Mode-locked Cr:ZnS Laser," in *Lasers, Sources, and Related Photonic Devices*, OSA Technical Digest (CD) (Optical Society of America, 2012), paper AW5A.5.

1. Introduction

Cr^{2+}-doped lasers of the II-VI family [1] operating between 2 and 3.5 μm [2] have recently matured to the commercial continuous-wave lasers, with the broadest among existing lasers amplification bandwidth $\Delta\lambda/\lambda$, making them a practical analogue to Ti:sapphire in the mid-IR wavelength range [3].

First reported as a gain-switched free-running pulsed source [1, 4], the Cr^{2+}:ZnS active medium has later been shown to operate in tunable continuous-wave regime [5], as diode-pumped [6], microchip [7], high-power [8], and tunable sources with over 1200 nm tuning range [9].

The Cr^{2+}:ZnS laser crystal is in many respects similar or even superior to Cr^{2+}:ZnSe. Having similar to Cr:ZnSe spectroscopic properties, it possesses a number of serious advantages. For practical applications, an important difference is that both absorption and emission bands of Cr:ZnS are shifted by ~100 nm to shorter wavelengths. The absorption band allows efficient pumping using widely available Er:fiber and InGaAsP-InP diode lasers in the 1.55−1.61 μm wavelength range, while the emission band moves towards the middle of the atmospheric water-free window around 2.3 μm, making the ultrashort-pulse operation at open air more stable and environmentally independent. The other important advantages include [5]: a noticeably higher than in Cr:ZnSe thermal conductivity in the cubic phase (27 W/mK in ZnS vs. 19 W/mK in ZnSe), the better hardness, better chemical and mechanical stability, lower level of toxicity, the higher thermal shock parameter (7.1 W/ $m^{1/2}$ in ZnS vs. 5.3 W/ $m^{1/2}$ in ZnSe), and the lower dn/dT (+ $46\cdot10^{-6}$ K^{-1} in ZnS vs. + $70\cdot10^{-6}$ K^{-1} in ZnSe). The third-order nonlinearity data are known with the lowest accuracy ($170\cdot10^{-20}$ m^2/W in Cr:ZnSe at 1.8 μm and $90\cdot10^{-20}$ m^2/W in Cr:ZnS at 1.3 μm [10]). Nevertheless, twice lower n_2 value in Cr:ZnS should allow higher energy femtosecond pulses from the oscillator. Altogether, the Cr:ZnS material holds an important promise of much better power and energy handling capability, while retaining comparable gain bandwidth and sufficiently high third-order nonlinearity. This makes Cr:ZnS attractive for both high-power and ultrashort pulse generation.

At the same time, technologically Cr:ZnS represents a challenge, especially what concerns the single-crystal materials. In particular, it exhibits tendency to polytyping and stacking

#178674 - $15.00 USD Received 26 Oct 2012; revised 26 Nov 2012; accepted 27 Nov 2012; published 12 Dec 2012

faults, resulting in inhomogeneous residual birefringence in the cubic phase [2]. Diffusion doping with chromium ions also takes more time and occurs at higher temperatures than in Cr:ZnSe due to the 300 degree difference in melting temperature. Therefore, diffusion of Cr ions into the lattice had to occur at either a higher temperature or for a significantly longer diffusion time period of a few days compared to ZnSe. Due to the availability of high-quality cubic Cr:ZnSe, this material was the first to demonstrate a femtosecond operation in a SESAM-controlled setup [11], followed by the Kerr-lens modelocked setups [12, 13], and recently by a directly diode-pumped realization [14]. Meanwhile, femtosecond Cr:ZnSe lasers have matured enough to be used in spectroscopic applications [15, 16], to seed an amplifier [17], and to pump a mid-IR OPO [18]. The initial attempts to mode-lock a Cr:ZnS laser resulted so far only in in ~1 ps pulses [19], partly because of the poor quality of the available crystal.

Nevertheless, based on the spectroscopic considerations above we anticipate that a Cr:ZnS laser would perform as good, if not better, than a Cr:ZnSe laser material, and should demonstrate better high-power handling capability. In this work we present the first femtosecond prismless Cr:ZnS laser operating in the water-free window around 2.3–2.4 μm and compare its performance with a single-crystalline Cr:ZnSe sample in the same cavity. This single-crystal based laser delivers up to 200 mW at fundamental wavelength, and can be operated in anomalous (solitonic) and normal (chirped-pulse) dispersion regimes. Demonstration of the mode-locked operation in the normal dispersion regime is especially important in the context of power scaling capability of Cr:ZnS.

2. Experimental setup

The ZnS sample was grown using physical vapor transport method and subsequently diffusion doped with Cr to a peak absorption coefficient of 6.1 cm^{-1} corresponding to Cr^{2+} concentration of about $6.10^{18}cm^{-3}$. The diffusion occurred in vacuum using CrS powder and heating to a temperature of 800–900°C for 2–3 days. The samples used were 3–5 mm in thickness with measured lifetime of 7.7 μs at room temperature.

The experimental setup is shown in Fig. 1. The active element was a 2.5 mm thick uncoated plate of Cr:ZnS at Brewster angle, providing 77% of pump absorption. Due to the polytyping, the sample possessed residual birefringence that could not be completely eliminated at any orientation, and that was inhomogeneous across the sample. This caused slight and position-dependent Lyot-filter effect, with a free spectral range >400 nm [9]. For comparison we also used a 2.8-mm long single-crystalline Cr:ZnSe with 63% pump absorption.

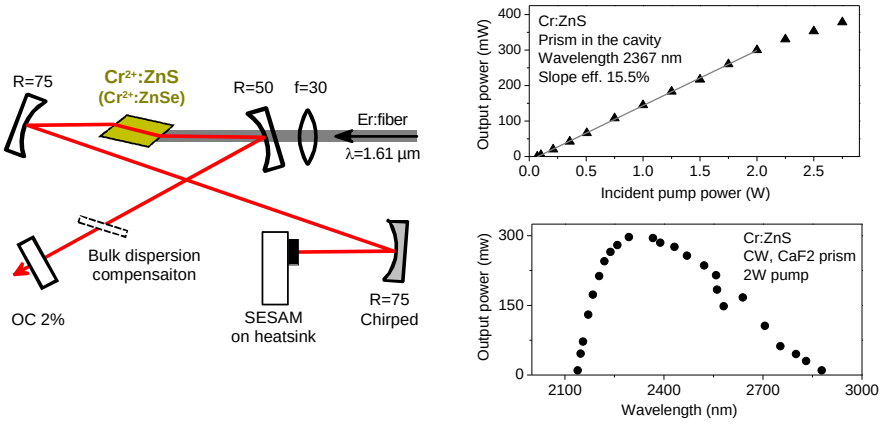

Fig. 1. Schematic diagram of the Cr:ZnS mode-locked laser and its characterization in continuous-wave operation without SESAM.

#178674 - $15.00 USD Received 26 Oct 2012; revised 26 Nov 2012; accepted 27 Nov 2012; published 12 Dec 2012

The saturable absorber mirror (SESAM) consisted of 50 layers of InAs/GaSb quantum wells, grown on top of a 15-pair GaSb/$AlAs_{0.08}Sb_{0.92}$ quarter-wave stack on a GaSb substrate [20]. The SESAM has been designed to provide small-signal absorption of 12% per bounce, relaxation time of 200-300 ps, and a saturation fluence of 40 μJ/cm^2. The SESAM was designed for 2450 nm central wavelength and its reflectivity band covered the range between 2250 and 2650 nm (Fig. 2(a)).

An X-fold cavity configuration with a SESAM was optimized for reliable self-starting. The astigmatically compensated cavity consisted of concave 75- and 50-mm r. o. c. mirrors, a folding 75-mm r. o. c. mirror, which focuses light into a 50 μm spot diameter on the SESAM, and a broadband plane-parallel 2% output coupler. The diode-pumped Er-fiber laser (IPG Laser GmbH, up to 5 W polarized output) was focused onto the crystal through the f = 30 mm lens. The Cr:ZnS crystal was edge-mounted on a copper block without additional cooling. For dispersion compensation we used z-cut sapphire or YAG plates of different thickness [11] and a chirped mirror [21] (Fig. 2(b), 2(c)). All measurements were performed at open air, with relative humidity 40-50%. The spectrum is analyzed by a commercial FTIR spectrometer. The pulse duration was measured using an autocorrelator based on a two-photon absorption in an amplified Ge photodetector. The laser output power was continuously monitored by a 15 MHz extended InGaAs detector, and the pulse train was monitored by a 2 GHz InGaAs TPA detector to exclude harmonic modelocking and drop-outs.

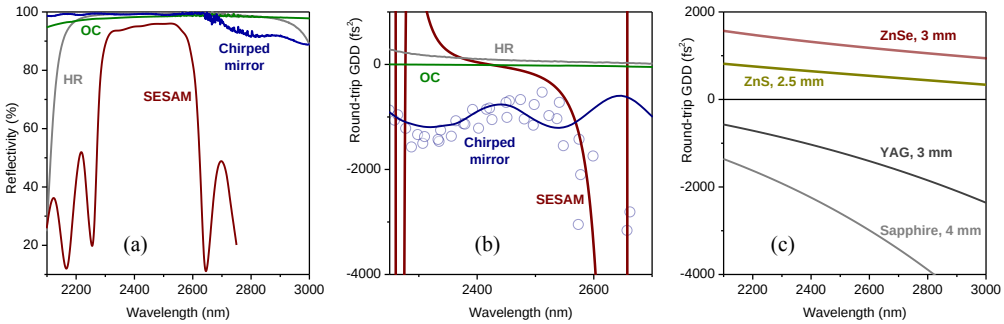

Fig. 2. Reflection spectra (a) and dispersion (b,c) of intracavity elements per round-trip. The dispersion data are calculated from known coating parameters and Sellmeier equations. The blue line and circles on graph (b) show the designed and measured dispersion of the chirped mirror, respectively, which agree within the measurement uncertainty in the wavelength range of 2250–2550 nm. OC: output coupler. HR: all high reflectors combined.

3. Results and discussion

Continuous-wave operation was characterized with a flat high reflector and a prism in the SESAM arm. The pump threshold and output power were measured to be 70 mW and 380 mW, respectively, with slope efficiency 15.5% and slight thermal roll-off above 2 W of pump power due to the lack of active cooling. Free-running wavelength was 2376 nm (2410 nm for Cr:ZnSe) and tuning range reached from 2150 to 2880 nm with ~450 nm FWHM at 2 W of pump power (Fig. 1). With a SESAM in place, the threshold pump power increased to ~160 mW as the SESAM provides the highest losses in the cavity (6%) and thus defines the threshold. Above the threshold, the laser would enter the Q-switched operation, but turn back to continuous-wave at about ~0.8 W of pump power. In an optimized configuration, the oscillator would support modelocked operation for about 1.2–2.2 W of pump power, self-starting above 1.6 W.

In the anomalous (soliton) dispersion regime, the laser routinely produced pulses of about 130 fs, corresponding to ~16 optical cycles (Fig. 3(a)) at the repetition rate of 180 MHz and output power up to 130 mW at 1.5 W of absorbed pump. The output spectrum of ~50 nm FWHM is centered around 2375 nm where calculated intracavity group-delay dispersion is

#178674 - $15.00 USD Received 26 Oct 2012; revised 26 Nov 2012; accepted 27 Nov 2012; published 12 Dec 2012

about −1000 fs^2. For comparison, Fig. 3(c) shows the output of a Cr:ZnSe laser where dispersion compensation has been accomplished by a 4-mm sapphire plate, but without a chirped mirror to provide comparable amount of about −1000 fs^2 at the gain peak. The pulse duration and spectral width are the same within the measurement error, while the output power is 90 mW at 1.4 W of absorbed pump, corresponding to ~30% lower efficiency with respect to Cr:ZnS sample.

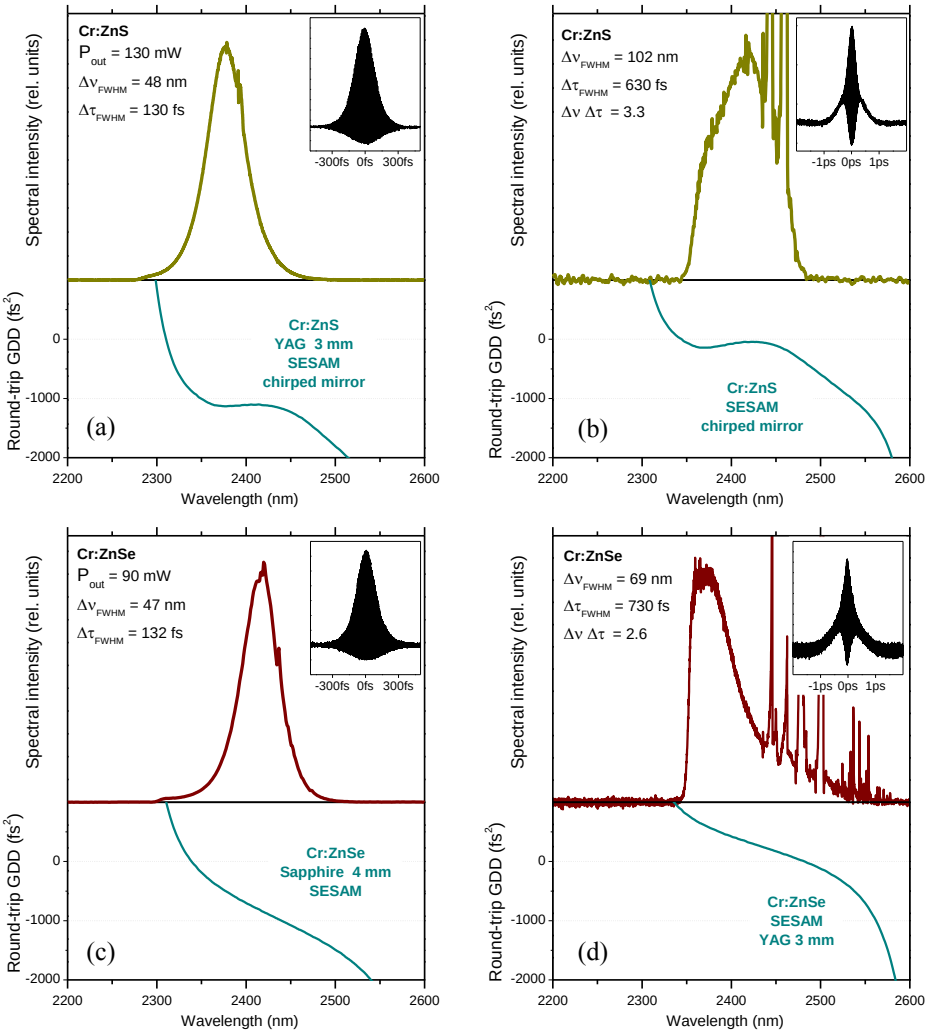

Fig. 3. Experimental spectra of Cr:ZnS and Cr:ZnSe lasers, operating in the anomalous (soliton) dispersion regime (a,c) and in the normal (chirped-pulse) dispersion regime (b,d). The insets show the corresponding autocorrelation traces, and the blue curves in the lower part show the corresponding round-trip dispersion, calculated by adding the dispersion data in Fig. 2(b,c) as listed in the subscripts. The uncertainty in the dispersion data originates mostly from the chirped mirror (Fig. 2(b)) and can be estimated as ±250 fs^2 for the curves (a) and (b).

The typical pulse train from the oscillator is plotted in the Fig. 4 showing good short-term pulse-to-pulse stability of the system. The pulse train clearly indicates that the laser operates at the cavity fundamental frequency without harmonic mode-locking. The pulse amplitude noise was estimated at ± 2%, defined to a significant part by the environmental influences. The modelocked regime could be sustained indefinitely long, but slow drifts of the uncooled setup required some readjustments every 30–60 min.

#178674 - $15.00 USD Received 26 Oct 2012; revised 26 Nov 2012; accepted 27 Nov 2012; published 12 Dec 2012

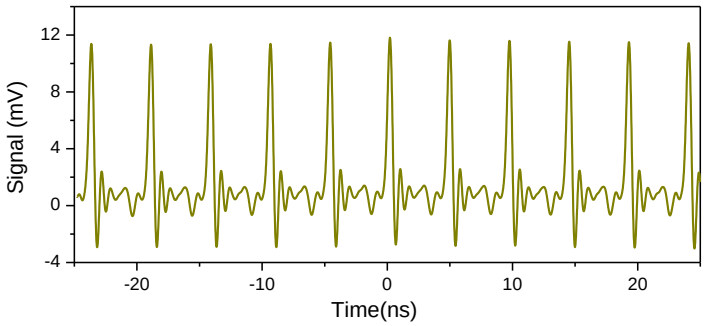

Fig. 4. The pulse train at the TPA photodiode from the mode-locked Cr:ZnS laser, operating in the anomalous (soliton) dispersion regime.

Removing the YAG plate brings the net GDD to nearly zero and resulted in a chirped-pulse regime with about 630-fs pulse duration. The output power could be scaled up to 205 mW at 1.9 W of absorbed pump (Fig. 3(b)). At this power level we observe leakage of 5-10% of energy into higher-order modes, visible as the narrow spectral lines in (Fig. 3(b)). This leakage was practically unavoidable at high pump power, reproduced itself in the chirped-pulse spectra of Cr:ZnSe sample as well (Fig. 3(d)), and was caused by the thermally-induced aberrations in the SESAM [22], where we could estimate the temperature raise to reach 50-70°C in the beam center. Further increasing the pump power resulted in more deterioration of the beam quality and loss of mode-locking stability, eventually followed by the SESAM damage.

In order to assess the prospects of the system let us revisit the loss, bandwidth and dispersion budgets (Fig. 2). It can be clearly seen that the SESAM has the narrowest bandwidth despite the quite high (for semiconductors) index contrast of 3.77 to 3.10 for the lattice-matched CaSb/AlAsSb stack. Moreover, the SESAM provides the main loss mechanism, and a major contribution to the higher-order dispersion. While it is relatively straightforward to decrease the losses of the SESAM and thus improve the efficiency of the system, any significant shortening of the pulse will be limited by the bottom mirror bandwidth. Moving further to few-cycle pulses with a SESAM will require special designs, such as e.g. hybrid semiconductor-metal [23], hybrid semiconductor-dielectric [3], or oxidized semiconductor stack [24]. The recently demonstrated Kerr-lens modelocked Cr:ZnS laser [25] is also free of the bandwidth limitation and allows increasing the pump power, but this comes at the expense of self-starting.

4. Conclusion

Summarizing, we have demonstrated the first SESAM-controlled femtosecond Cr:ZnS laser, generating high power 130 (205) mW stable 130 fs (630 fs) pulses at 180 MHz repetition rate in the soliton (chirped-pulse) regime. The Cr:ZnS crystal produced about 30-50% higher average power than a comparable Cr:ZnSe sample, but the overall system performance and limitations are defined by the SESAM device, rather than by the active medium choice. Taking full advantage of the Cr:ZnS bandwidth and high-power capability would require a saturable absorber with lower initial absorption, significantly broader reflection band and well-controlled dispersion.

Acknowledgments

This work was supported by the Austrian Science Fund (FWF) project P-17973, the Norwegian Research Council (NFR) project FRITEK/191614, and the Nano2021 project N219686.

#178674 - $15.00 USD Received 26 Oct 2012; revised 26 Nov 2012; accepted 27 Nov 2012; published 12 Dec 2012